Asian Journal of Plant Sciences

ISSN 1682-3974

science alert

ANSInet
an open access publisher
http://ansinet.com

Asian Journal of Plant Sciences 11 (1): 9-18, 2012
ISSN 1682-3974 / DOI: 10.3923/ajps.2012.9.18

Vegetation Cover Assessment Based on Soil Properties in Arid and Semi-arid Areas using Landsat Images: A Case Study in Neyshaboor Area

[1]M. Ghaemi, [2]S.H. Sanaeinejad and [1]A. Astaraei
[1]Department of Soil Science,
[2]Department of Water Engineering, Ferdowsi University of Mashhad, Iran

Abstract: Remote sensing is generally accepted as a powerful technique for land surface studies in arid and semi-arid regions. This technique is also very useful for other environmental studies such as shallow and undeveloped soil properties. In this research, band relations and principal component analysis were utilized to develop an appropriate model for vegetation cover monitoring and also finding a relation between vegetation cover and soil properties according to Digital Number of pixels in the LandSat image. The relations between spectral values of the pixels with the parameters were analyzed in order to develop a statistical model. The model was also assessed by a regression analysis and comparing of R-Square coefficients for each of the variables. Two different series of corresponding digital numbers for vegetation cover were distinguished and categorized into 40 and 70 samples. Different indices and band combinations were used for a regression stepwise analysis. The results showed that bands 1, 2 and 3 with R-Square 0.26, 0.33 and 0.38, respectively showed higher correlation than other spectrum bands. Other indices such as brightness analysis, greenness component, tasseled cap and PCA showed higher correlations. The highest R-square statistically significant at 95% confidence level was derived when vegetation cover data and DN in different band compositions were considered in the regression analysis. Radiation reflection varies with soil properties and other soil factors depending on vegetation cover density; therefore, estimation of vegetation cover based on remote sensing data is very complicated. However, this study showed that ETM+ images are very useful for monitoring vegetation spatial variability especially in remote arid and semi-arid areas.

Key words: Vegetation cover, soil properties, remote sensing, landsat NDVI

INTRODUCTION

More than one third of world's soils are located in arid and semi-arid area such as in Iran. Most soils in these areas are saline which affects the other soil properties and consequently vegetation cover. Vegetation cover map is essential for land management and land developing plans. Collecting, accessing and updating field data in either aerial or global scale is a difficult task. These types of data are traditionally collected from small areas in different time scales thus providing different accuracy and validity. Consequently, it is not easy to use them as an appropriate data collection procedure for scientific studies (Pettorelli *et al*., 2005). To overcome these problems researchers widely use remote sensing data to study vegetation cover (Mokhtari *et al*., 2000; Huete, 2004). Remote sensing technique is more useful in terms of spatial and temporal resolution and more accurate than traditional methods and thus could save time and money. Changes in vegetation cover and density is affected by soil properties such as soil salinity, soil water content and soil mineral availability which in reflected by soil spectral responses in the images (Barnes *et al*., 2003). Recently, spectrometry and spectrum relations recorded from different land covers have been used increasingly by different researchers to study natural resources, especially vegetation cover in aerial (consider changing "aerial" to "local") and global scales. These indices show a good correlation with vegetation cover; however spectrum reflectivity varies with sun elevation, sun aspect, soil background and atmospheric conditions (Aitkenhead and Aalders, 2008).

The main problem in arid and semi-arid areas is vegetation scarcity. The effect of vegetation cover in the reflected spectrums recorded by satellite sensors is low when vegetation cover is less than 26% (Taherkia, 1996). Also, when green cover is about 10%, weak absorption in infra-red spectrum resulting from bare soil and its containing minerals could cause darkness in the image. On the other hand when vegetation cover is more than 60%, it is hard to recognize soil spectrum reflections (Huete, 1989).

Corresponding Author: M. Ghaemi, Department of Soil Science, Ferdowsi University of Mashhad, Iran
Tel: +98 511 8795612 Fax: +98 511 8787430

In a research conducted in Pakistan, different indices such as soil deficit index, vegetation index and Principal Component Analysis (PCA) were used to study the relations between soil parameters and satellite images. The results showed that Salinity Index (SI), Normalized Differential Salinity Index (NDSI) and Brightness Index (BI) had more correlation with the image data in saline soils. NDSI and Ratio Index (RI) were low in high saline soils, showing a week vegetation cover (Khan *et al*., 2001). Experimental models describe relations between biophysics measurements and remote sensing data, providing useful information about biomass, trees coverage and Leaf Area Index (LAI). The most common regression analysis in this field use Soil Vegetation Index (SVI) which is derived from near infrared and red spectrum reflections of an image (Cohen *et al*., 2003).

Developing a suitable model for vegetation cover depends on environmental conditions which in turn depend on healthiness and greenness of vegetations. This research uses digital values of satellite images and vegetation cover data collected from the study area in a multi-regression analysis to develop a statistical model for monitoring and studying of vegetation cover in a typical arid and semi-arid area, Neyshaboor in the North-East of Iran. The potential of ETM+ images for studying soil organic materials where the vegetation cover is sparse was also investigated.

MATERIALS AND METHODS

General features of the study area: The study area is located in the Neyshaboor plain in Khorasan-Razavi province in the North-East of Iran, geographically located between Longitudes 58.57 to 59.13 and Latitudes 35.85 to 36.25. The climate is arid to semi-arid with annual average temperature of 14.5 and precipitation of 250 mm based on Ambergeh climate classification method. According to land-use maps, this area is generally saline with agricultural activities.

LandSat ETM+ image including 6 spectrum bands with 30 m resolution, one thermal band with 60 m resolution and panchromatic band with 15 meters resolution from track 160 and row 35 taken in 10th of July 2002 was used. The image was originally corrected for general geometric and radiometric errors.

General aspect of the analysis: However, more geometrical corrections were also applied for more confidence. Different image processing techniques were used including image enhancement, PCA, tasseled cap transformation and also 50 vegetation indices derived from the reflected bands. Some of the indices are listed in Table 1. The ETM+images were converted into an appropriate format to be used in ERDAS Imagine 8.6 and IDRISI Kilimanjaro software.

Field work: After preprocessing of the image its general features were compared with the corresponding land use map (scale: 1/250000). A part of Neyshaboor plane with 765 km^2 was selected based on soil properties and vegetation cover estimated from field observations. The area is contained in a 1881×1497 pixels in the image. The area was divided into three main parts depending on their salinity determined from land use map and field observations. A mesh with 10×50 grids was drawn with 1000 m grid length on the area (Fig. 1). One hundred of

Table 1: Some of the principal and artificial bands used in this research

Index name	The equation	Reference
Near Inferared Ratio (NIR)	TM4/TM3	Pettorelli *et al.* (2005)
Leaf water content (Mid- IR-Index)	TM5/TM7	Pettorelli *et al.* (2005)
Normalized difference vegetation index	(TM4-TM3)/(TM4+TM3)	Foody *et al.* (2001)
Transformed vegetation index	(TM5-TM3)/(TM5+TM3)	Pettorelli *et al.* (2005)
Reflectance absorption index	TM4/(TM3+TM5)	Arzani and King (2008)
Modified normalised difference	(TM4-(1.2×TM3)/(TM4+TM3)	Pettorelli *et al.* (2005)
PD321	TM3-TM2	Arzani and King (2008)
PD311	TM3-TM1	Arzani and King (2008)
MIRV1	(TM7-TM3)/(TM7+TM3)	Leblon (1993)
DVI	TM4-TM3	Foody *et al.* (2001)
MIRV2	(TM5-TM3)/(TM5-TM3)	Arzani and King (2008)
Green vegetation index	-0.29 (G) -0.56(R)+0.6(IR)+0.49(IR)	Leblon (1993)
SAVI	[NIR-RED)/(NIR+RED+L)] × (1+L)	Pettorelli *et al.* (2005)
GEMI	ç× (1-0.25×ç)-(Red-0.125) / (1-Red)	Nikolakopoulos (2003)
OSAVI	(NIR -Red) / (NIR + Red + 0.16)	Nikolakopoulos (2003)
Stress-related	(TM1×TM2)/TM3	Foody *et al.* (2001)
Normalized-based	(TM4 - (TM1 + TM2))/(TM4 + (TM1 + TM2))	Foody *et al.* (2001)
PCA1	Derived from principal components of bands 1,2 and 3	Bhatti *et al.* (1991) and Frazier and Cheng (1989)
PCA2	Derived from principal components of bands 4,5 and 7	Bhatti *et al.* (1991) and Frazier and Cheng (1989)
PCA3	Derived from principal components of bands 1,2 3 5, 7 and 4	Bhatti *et al.* (1991) and Frazier and Cheng (1989)
Brightness	Brightness derived from tasseled cap	Bhatti *et al.* (1991) and Frazier and Cheng (1989)
Greenness	Greeness band derived from tasseled cap	Bhatti *et al.* (1991) and Frazier and Cheng (1989)
Wetness	Humid bands derived from tasseled cap	Bhatti *et al.* (1991) and Frazier and Cheng (1989)

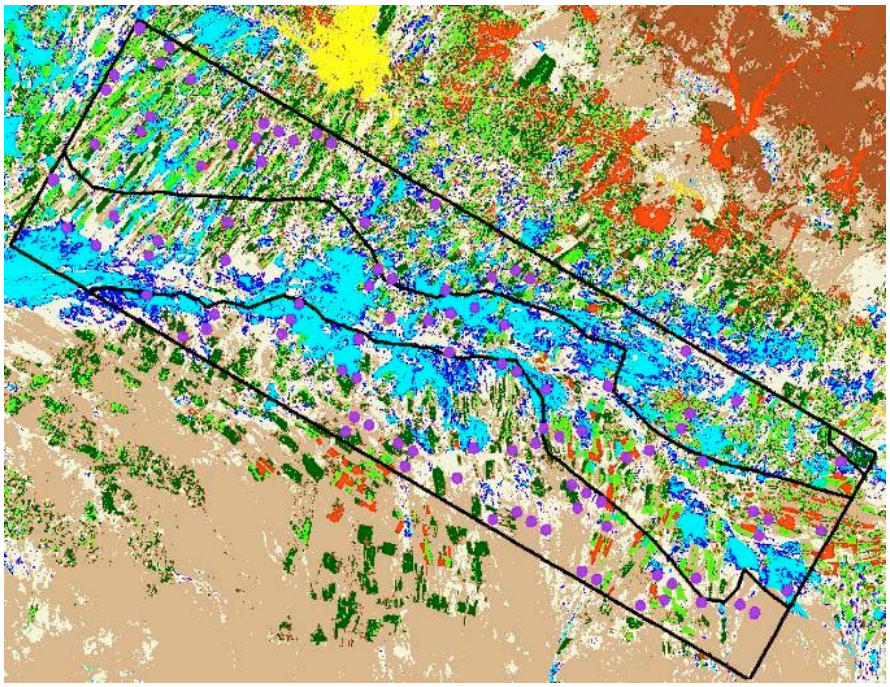

Fig. 1: The frame clipped from the original ETM+ image for the study area and the position of random locations for sampling points

the grids were randomly selected and 3 separate points 100 m apart were chosen in each selected grid as sampling points. A sample soil (20×20 cm surface and 20 cm depth) was recovered from each sampling point. The geographic position was recorded by a Garmin GPS and the samples transported to a soil laboratory for testing.

The percentage of vegetation cover was determined by randomly throwing a 50×50 cm quadrant around each sampling point three times. Other land use characteristics were also recorded based on on-site field observation. According to these observations, high percentage vegetation cover was assigned to farm lands. Medium and low vegetation cover or bare soil was considered as natural vegetation cover. Eventually, the data collected was integrated as an assessment of vegetation cover.

Measuring of soil physical and chemical properties: The recovered sample soils were air dried and then sieved through a 2 mm sieve for laboratory testing. Different parameters were measured including soil acidity by using a pH meter, EC in soil saturation extracts was measured by EC meter equipment, soil organic carbon (SOC) was determined by Walkley and Black (1934), Cation Exchange Capacity (CEC) was determined by Chapman (1965) method and soil particles size was determined by standard hydrometer method (Gee and Bauder, 1986).

Statistical tests: Statistical software JMP4 was used for the statistical analysis. The R-Square for correlation equation between the percentage vegetation cover and the DN values in the corresponding pixels were compared for different bands and indices and the most suitable variables were selected for the multi regression analysis in a stepwise method. All the coefficients were considered statistically significant at 95% confidence level.

RESULTS AND DISCUSSION

The R-Square was low when all of the data from the low to high salinity soil samples were considered in the regression analysis (Table 2). The regression coefficient was considered statistically significant at 95% confidence level. However, bands 1, 2 and 3 with R-Square 0.26, 0.33 and 0.38 respectively showed higher correlation than other spectrum bands. Other indices such as brightness analysis, greenness component, tasseled cap and PCA (PCA1 PCA3, BI1, SI, VI5, VI1, VI6 and RI) showed even higher correlations.

Table 2: The equations and their corresponding R-Square for vegetation cover and soil (applying all the data set)

Index name	R^2	Index name	R^2
Band 1	0.26	Band 4	0.30
Band 2	0.33	Band 5	0.20
Band 3	0.38	Band 7	0.18
PCA1	0.33	Brightness	0.30
PCA	0.16	Greenness	20.31
PCA3	0.30	Wetness	0.12
PD311	0.07	VNIR1	0.03
PD321	0.04	VNIR2	0.04
Stress-Related	0.01	NDVI	0.04
Normalized-Based	0.05	TVI	0.04
IPVI	0.05	IR	0.05
OSAVI	0.04	IR2	0.05
BI1	0.06	MND	0.04
SI	0.16	MINI	0.05
RI	0.05	DVI	0.04
MSAVI	0.04	Complex Division2	0.10
BI2	0.05	GVI	0.04
VI1	0.04	NDSI	0.13
VI5	0.02	RA	0.10
VI6	0.01	SAVI	0.04
MSI	0.06	COSRI	0.04
MSR	0.02	RATIO	0.04

The data is sorted based on the trends which could be seen among some sample data in the graphs (Fig. 2). Two groups of data with 70 (series 1) and 40 (series 2) samples in each of them were categorized from the total data set. Figure 3 shows the results from data series 1 with 72 sample data. There is an obvious trend which can be seen in all of the graphs. The results from data series 2 showed a similar trend as is shown in Fig. 4.

It was found from the corresponding field data that data series 2 belongs to lands where salinity varies from low to medium (maximum up to 9 dS m^{-1}) covered by vegetation classified as ranging from low to medium, mostly containing loam and loam-sandy soils. The land was used for horticulture and agriculture purposes with 0.3 to 1% of organic materials.

The data series 2 mostly located in agriculture lands with loam-sand and loam soils, high density vegetation cover (40 to 100%), none or low salinity (3.83 dS m^{-1}) and 0.9 to 1.6 organic materials. Statistical analysis showed a higher R-Square between the independent variables and vegetation cover for both of the data series in comparison to the whole data set. The results are shown in Table 3 and 4.

In this analysis we used stepwise regression method to obtain a suitable model which can explain the relation between vegetation and soil indices with image data for the whole data set. Figure 2 shows the scattering diagrams for vegetation cover percentage against the corresponding DNs. Equation 1 is a typical derived model from this analysis:

$$Veg = 228.29 + 1.67\ b3 \quad (1)$$

Table 3: The equations and their corresponding R-Squares for data series 1

Index	R^2	Index	R^2
Band 1	0.44	Band 4	0.32
Band 2	0.50	Band 5	0.50
Band 3	0.54	Band 7	0.32
PCA1	0.41	Brightness	0.45
PCA2	0.33	Greenness	0.30
PCA3	0.44	Wetness	0.30
PD311	0.50	VNIR1	0.10
PD321	0.43	VNIR2	0.20
Stress-Related	0.20	NDVI	0.23
Normalized-Based	0.13	TVI	0.30
IPVI	0.13	IR	0.24
OSAVI	0.23	IR2	0.20
BI1	0.50	MND	0.23
SI	0.50	MINI	0.20
RI	0.45	DVI	0.30
MSAVI	0.30	Complex Division2	0.20
BI2	0.51	GVI	0.20
VI1	0.20	NDSI	0.23
VI5	0.31	RA	0.10
VI6	0.31	SAVI	0.23
MSI	0.26	COSRI	0.24
MSR	0.20	RATIO	0.30

In which Veg is vegetation cover in percentage and b3 is Digital Number (DN) of band 3 from ETM+. The R-square is 0.38 and RMSE = 33.17 for this equation. This R-Square is not very good and the high value for RMSE also shows that the percentage of vegetation cover is highly varied over the area.

The highest R-square statistically significant at 95% confidence level was derived when vegetation cover data and DN in different band compositions were considered in the regression analysis. The highest R-squares are for the main bands of 1, 2, 3, 4, 5, RI, SI, BI1, BI2, PD311, PCA1, PCA3 and brightness components in group one and also for bands 2,3, RI, SI, BI1, MSAVI, COSRI, VI5, PCA1 and brightness components in group two.

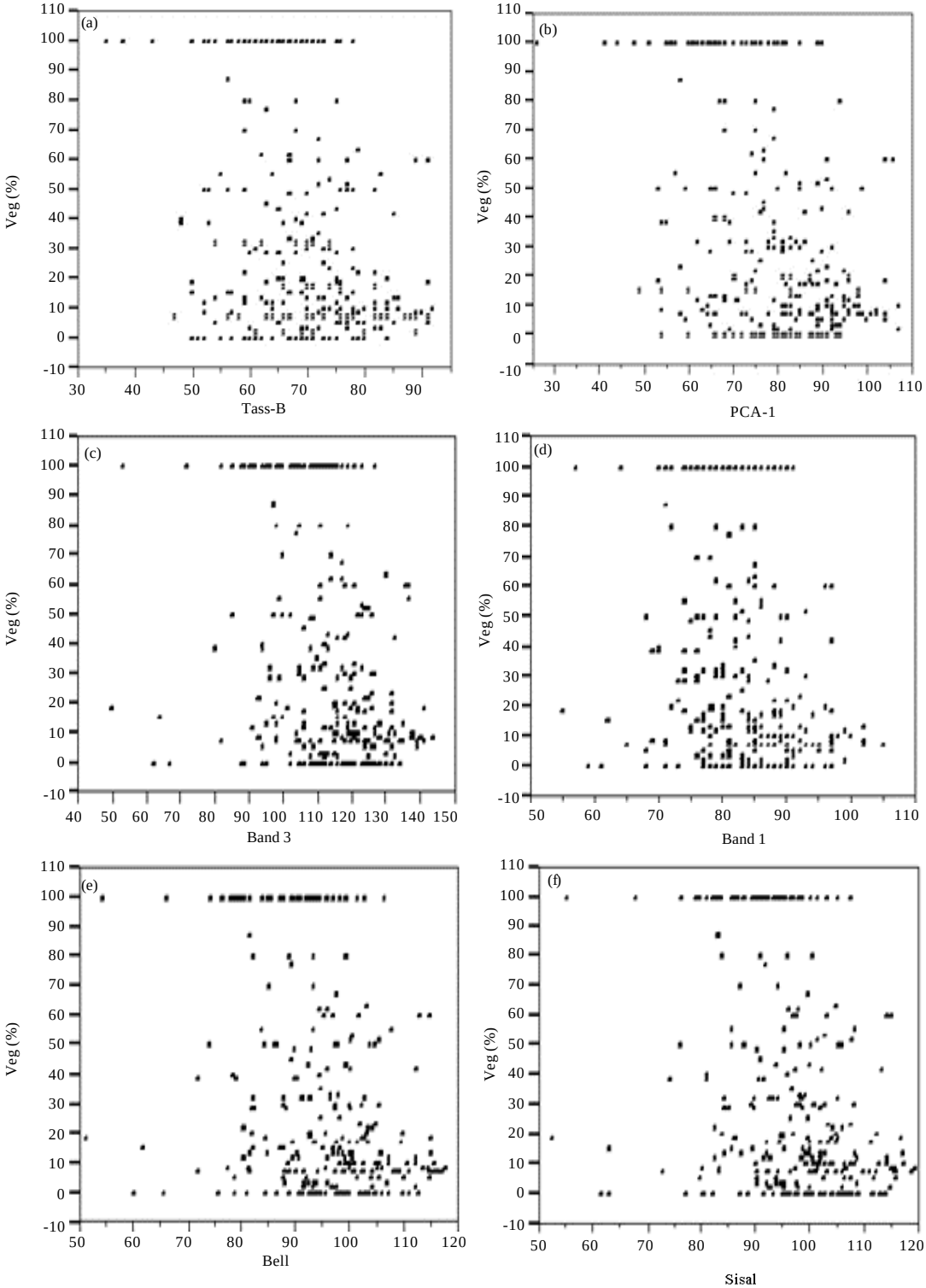

Fig. 2(a-f): Scattering diagram for vegetation cover percentage against corresponding DNs in ETM+pixels (For all the data set)

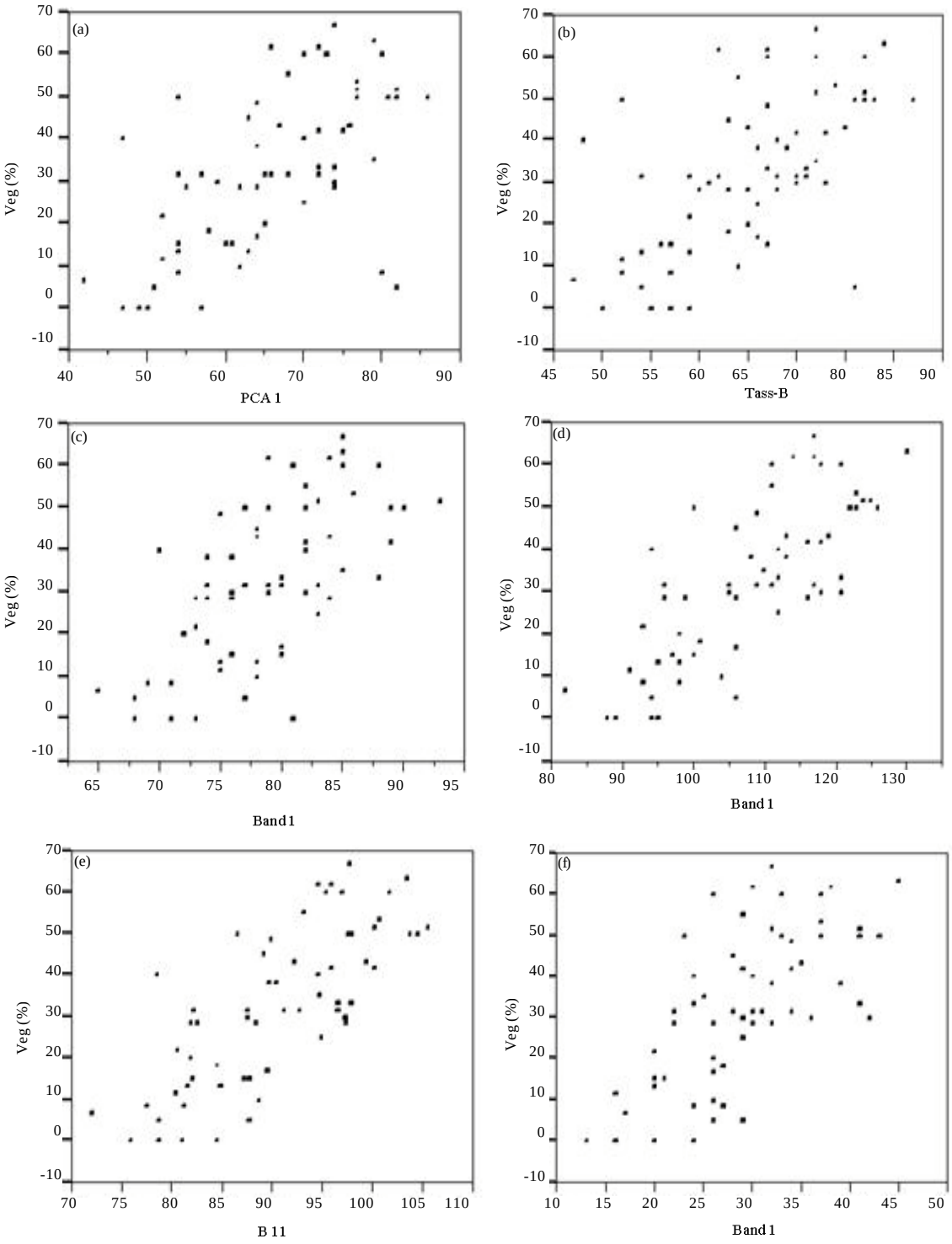

Fig. 3(a-f): Scattering diagram showing percentage of vegetation cover against DN of the corresponding pixel in the image (data series 1)

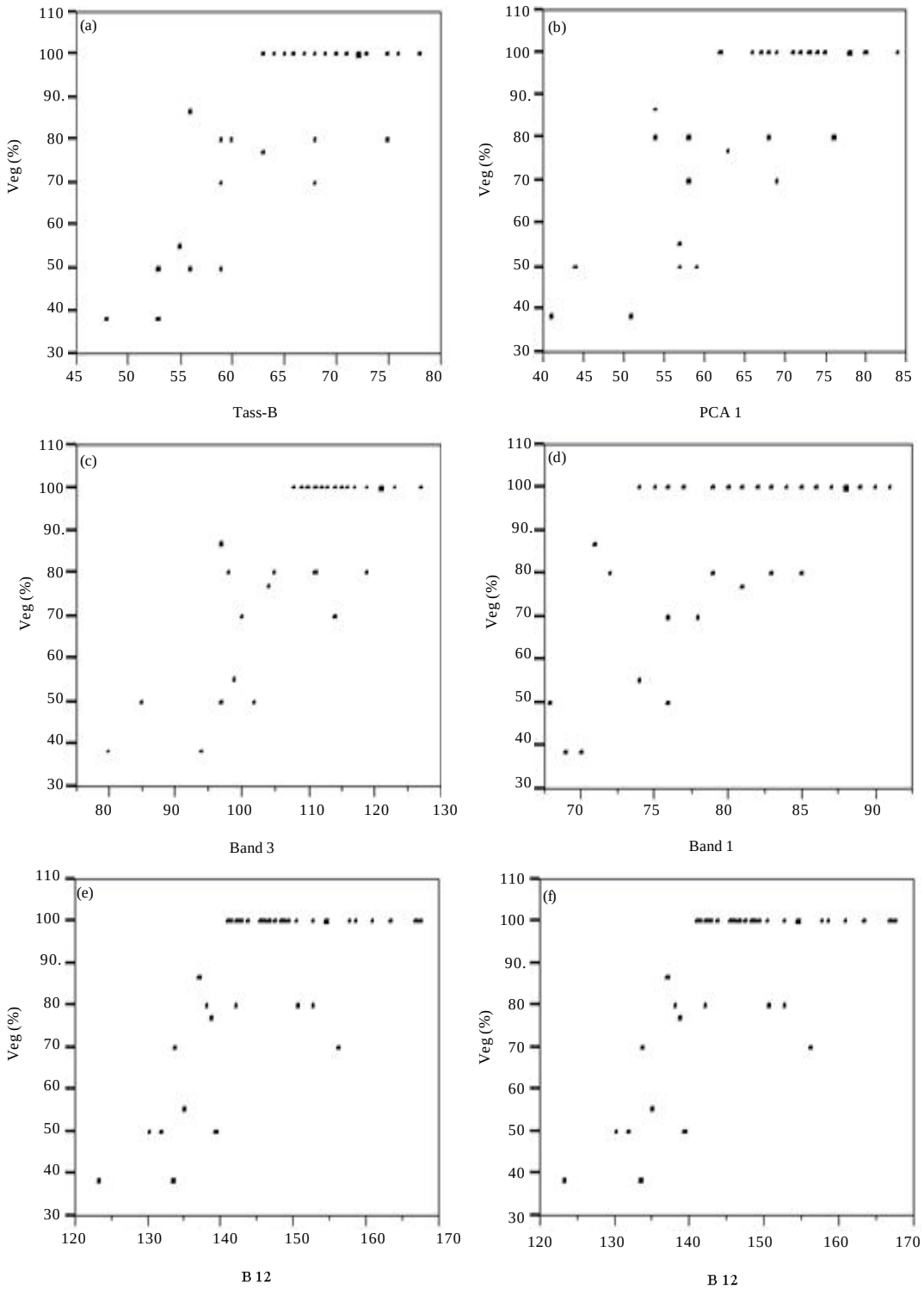

Fig. 4(a-f): Scattering diagram showing percentage of vegetation cover against DN of the corresponding pixel in the image (data series 2)

Table 4: The equations and their corresponding R-Squares for data series 2

Index	R^2	Index	R^2
Band 1	0.42	Band 4	0.32
Band 2	0.55	Band 5	0.38
Band 3	0.63	Band 7	0.18
PCA1	0.61	Brightness	0.57
PCA2	0.35	Greenness	0.32
PCA3	0.51	Wetness	0.16
PD311	0.41	VNIR1	0.10
PD321	0.47	VNIR2	0.20
Stress-Related	0.20	NDVI	0.35
Normalized-Based	0.14	TVI	0.33
IPVI	0.33	IR	0.14
OSAVI	0.35	IR2	0.10
BI1	0.60	MND	0.34
SI	0.59	MINI	0.10
RI	0.43	DVI	0.34
MSAVI	0.44	Complex Division2	0.20
BI2	0.43	GVI	0.20
VI1	0.30	NDSI	0.35
VI5	0.43	RA	0.34
VI6	0.30	SAVI	0.35
MSI	0.15	COSRI	0.42
MSR	0.35	RATIO	0.34

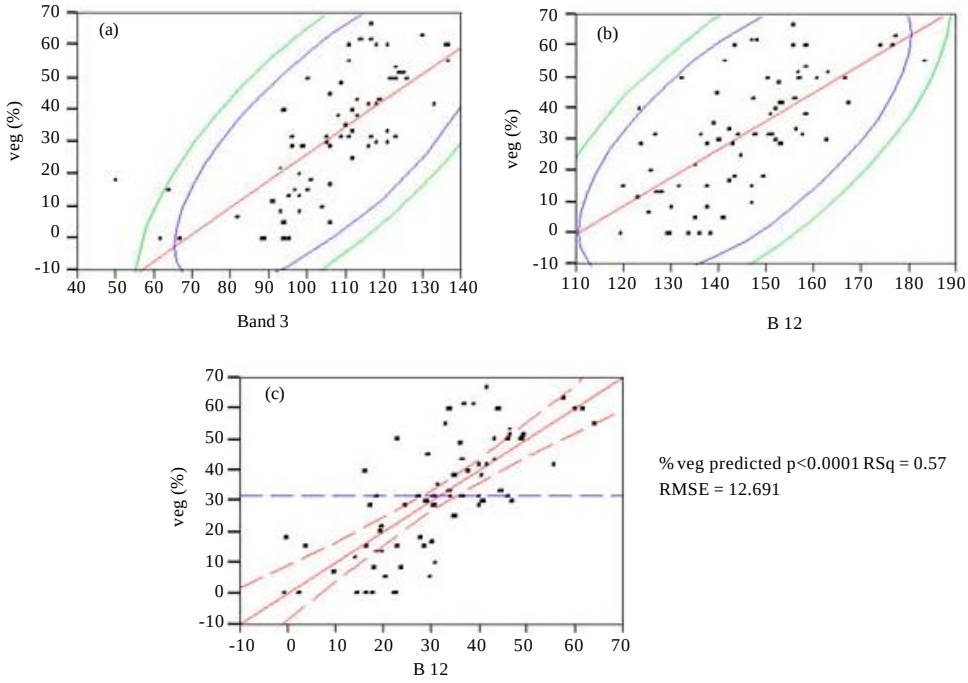

Fig. 5(a-c): The corresponding scattering diagram between percentage of vegetation cover and DN values in band 3 and BI2 analyzed by equation 2 for the data series 1

The R-squares for vegetation cover are low because the background effect of soil is dominant in arid and semi-arid areas and also because reflections from vegetation cover is naturally nonlinear (Schmidt and Karnieli, 2001; Sellers *et al*., 1992). When the data from the special trends appearing in the graphs were separated, the R-Square increased showing the effect of physical and chemical properties of soil on vegetation reflections. Figure 5 and 6 show the scatter diagram of vegetation cover with different bands and indices which are

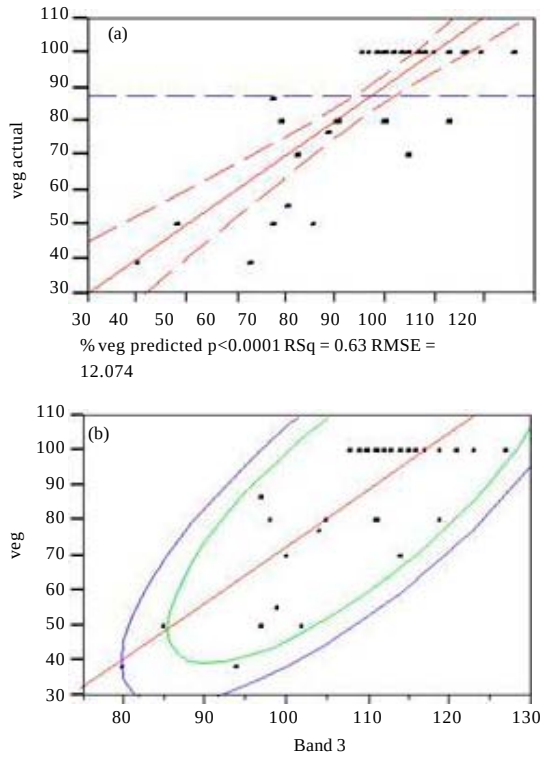

Fig. 6(a-b): The corresponding scattering diagram between percentage of vegetation cover and DN values in band 3 analyzed by equation 2 for the data series 1

separated from the main data set in the two data series. As can be seen, all of the separated data are located in 95% area in both series.

The models illustrated by the equations 2 and 3 give the best results for estimating low density vegetation cover in the study area among all of the other models that were examined in this analysis. This is especially true when the study area is classified into different homogeneous districts. The models can be used to study the response of vegetation cover to environmental factors such as salinity in large scale areas:

$$Veg = -86.12+0.37\ BI2+0.6\ b3 \quad (2)$$

$$R\text{-Square} = 0.57 \text{ and } RMSE = 12.69\ Veg = -88.46 +1.6\ b \quad (3)$$

$$R\text{-Square} = 0.63 \text{ and } RMSE = 12.07$$

where Veg is vegitation cover in percentage and BI2 and b3 are as explained before.

The coefficients show that using indicators such as vegetation indices and enhancement techniques such as PCA in the analysis can increase the R-square value in comparison to using main bands. The regression analysis of PCA and vegetation indices showed good results in monitoring of vegetation cover in saline lands. Dwivedi and Sreenivas (1998) also showed similar results. The index of BI2 which was derived from bands 3 and 4 is suitable for determining the spatial changes in vegetation cover where the highest vegetation reflection is recorded by satellite. This is also reported by Guo *et al.* (2000).

It can be concluded from the results that models illustrated by the equations 2 and 3 gives the best results for estimating low density vegetation cover in the study area among all of the other models that were examined in this analysis. This is especially true when the study area is classified into different homogeneous districts (Huete, 1996). The models can be used to study the response of vegetation cover to environmental factors such as salinity in large scale areas (Hickler *et al.*, 2004).

CONCLUSION

It is concluded that all of the examined indices have some capabilities of showing different aspects of the surface conditions under different environmental conditions.

Different band combinations, different indices and also image enhancement and analysis can be used for estimating land cover, if climate conditions, land use, soil salinity and its spatial variability, soil properties and other factors in each area are considered carefully.

Radiation reflection varies with soil properties and other soil factors depending on vegetation cover density; therefore estimation of vegetation cover based on remote sensing data is very complicated. However, this study showed that ETM+ images are very useful for monitoring vegetation spatial variability especially in remote arid and semi-arid areas where collecting field data is very difficult and even impossible in some situations. It is recommended to further examine the results in other areas to ascertain the most suitable ones for surface monitoring.

ACKNOWLEDGMENTS

We would like to thank Remote Sensing Unit of Ferdowsi University of Mashhad for their help for doing this study.

REFERENCES

Aitkenhead, M.J. and I.H. Aalders, 2008. Classification of landsat thematic mapper imagery for land cover using neural networks. Int. J. Remote Sensing, 29: 2075-2084.

Arzani, H. and G.W. King, 2008. Application of remote sensing (Landsat TM data) for vegetation parameters measurement in Western division of NSW. International Grassland Congress. Hohhot, China. ID No. 1083.

Barnes, E.M., K.A. Sudduth, J.W. Hummel, S.M. Lesch and D.L. Corwin *et al*., 2003. Remote and ground-Based sensore techniques to map soil properties. Photogramm. Eng. Remote Sensing, 69: 619-630.

Bhatti, A.U., D.J. Mulla and B.E. Frasier, 1991. Estimation of soil properties and wheat yields on complex eroded hills using geostatistics and thematic mapper images. Remote Sens. Environ., 37: 181-191.

Chapman, H.D., 1965. Cation Exchange Capacity. In: Methods of Soil Analysis, Part 2, Black, C.A. (Ed.). American Society Agronomy, Madison, WI., USA., ISBN-10: 0891180729, pp: 891-901.

Cohen, W.B., T.K. Maiersperger, S.T. Gower and D.P. Turner, 2003. An improved strategy for regression of biophysical variables and landsat ETM+ data. Remote Sensing Environ., 84: 561-571.

Dwivedi, R.S. and K. Sreenivas, 1998. Delineation of salt-acted soils and waterlogged areas in the indo-gangetic plains using IRS-1C LISS-III data. Int. J. Remote Sensing, 19: 2739-2751.

Foody, G.M., M. Cutler, J. Mcmorrow, D. Pelz, H. Tangki, D.S. Boyd and I. Douglas, 2001. Mapping the biomass of Bornean tropical rain forest from remotely sensed data. J. Global Ecol. Biogeogr., 10: 379-387.

Frazier, B.E. and Y. Cheng, 1989. Remote sensing of soils in the Eastern Palouse region with landsat thematic mapper. Remote Sensing Environ., 28: 317-325.

Gee, G.W. and J.W. Bauder, 1986. Particle Size Analysis: Methods of Soil Analysis. 2nd Edn., ASA-SSSA, Madison, WI.

Guo, X., K.P. Price and J.M. Stiles, 2000. Modeling biophysical factors for grasslands in Eastern Kansas using landsat TM data. Trans. Kansas Acad. Sci., 103: 122-138.

Hickler, T., B. Smith, M.T. Sykes, M.B. Davis, S. Sugita and K. Walker, 2004. Using a generalized vegetation model to simulate vegetation dynamics in Northeastern USA. Ecol. Soc. Am., 85: 519-530.

Huete, A.R., 1989. Soil Influences in Remotely Sensed Vegetation Canopy Spectra. In: Theory and Applications of Optical Remote Sensing, Asrar, G. (Ed.). John Wiley and Sons, New York, USA., ISBN-13: 9780471628958, pp: 107-141.

Huete, A.R., 1996. Extension of soil spectra to the satellite: Atmosphere, geometric and sensor considerations. Photointerpretation, 34: 101-114.

Huete, A.R., 2004. Remote Sensing of Soils and Soil Processes. In: Remote Sensing for Natural Resources Management and Environmental Monitoring: Manual of Remote Sensing, Ustin, S. (Ed.). 3rd Edn. John Wiley and Sons Inc., New York, USA., pp: 1-48.

Khan, N.M., V.V. Rastoskuev, E.V. Shalina and Y. Sato, 2001. Mapping salt-affected soils using remote sensing indicators: A simple approach with the use of GIS IDRISI. Proceedings of the 22nd Asian Conference on Remote Sensing, November 5-9, 2001, Singapore, pp: 1-5.

Leblon, B., 1993. Soil and Vegetation Optical Properties. In: Applications in Remote Sensing, Volume 4, The International Center for Remote Sensing Education (Ed.). John Wiley and Sons Ltd., New York.

Mokhtari, A., S. Feiznia, H. Ahmadi, S.J. Khajehdin and F.A. Rahnama, 2000. Application of remote sensing in preparation data layers of land use and land cover in MPSIAC soil erosion model. J. Res. Establishment, 46: 82-87.

Nikolakopoulos, K.G., 2003. Use of vegetation indexes with aster viner data for burnt areas detection in Western Peloponnese, Greece. Remote Sensing Laboratory, Panepistimiopolis, Athens, Greece.

Pettorelli, N., J.O. Vik, A. Mysterud, J.M. Gaillard, C.J. Tucker and N.C. Stenseth, 2005. Using the satellite-derived NDVI to assess ecological responses to environmental change. Trends Ecol. Evol., 20: 503-510.

Schmidt, H. and A. Karnieli, 2001. Sensitivity of vegetation indices to substrate brightness in hyperarid environment: The Makhtesh Ramon Crater (Israel) case study. Int. J. Remote Sensing, 17: 3503-3520.

Sellers, P.J., J.A. Berry, G.J. Collate, C.B. Field and F.G. Hall, 1992. Canopy reflectance, photosynthesis and transpiration III. A reanalysis using improved leaf models and a new canopy integration scheme. Remote Sensing Environ., 42: 187-216.

Taherkia, H., 1996. Remote Sensing. Tehran University, Tehran, Iran, pp: 128-150.

Walkley, A. and I.A. Black, 1934. An examination of the degtjareff method for determining soil organic matter and a proposed modification of the chromic acid titration method. Soil Sci., 37: 29-38.